Quantum Electronics **52** (6) 555–559 (2022)

https://doi.org/10.1070/QEL18061

Characteristics of a heterodyne laser interferometer laboratory model for the development of a space gravimetry project

K.S. Kudeyarov, V.K. Milyukov, D.S. Kryuchkov, I.A. Semerikov,
O.A. Ivlev, K.Yu. Khabarova, N.N. Kolachevsky

Abstract. **We investigate displacement measurements of up to 17 μm on a heterodyne laser interferometer laboratory model. The measurement error for small (up to 200 nm) linear displacements is found to be 270 pm at a 10-s averaging time. The results obtained can be used for developing a space laser interferometric system for the global Earth's gravity field mapping.**

Keywords: *space gravimetry, laser interferometer, linear displacement measurements.*

1. Introduction

The accuracy of determining parameters of the Earth's gravity field and its variation in time and space is enhanced by employing clusters of spacecrafts (SCs), which form a kind of an 'orbital gradiometer'. Such a scheme makes it possible to efficiently suppress coherent disturbances acting on the SCs and measure variations of the Earth's global gravity field. The first satellite constellation, which comprised two SCs in near-circular orbits at ∼500-km altitude separated from each other by a distance of ∼200 km, was launched in the frameworks of the special gravitational mission GRACE (Gravity Recovery and Climate Experiment) intended for mapping the Earth's global gravity field with a spatial resolution of ∼400 km every thirty days. The satellites were launched on 17 March 2002 [1]. The spacecrafts were linked by a high-accuracy inter-satellite microwave K-band ranging system. For obtaining the required accuracy of an inter-satellite distance, the dual-frequency K- (24 GHz) and K_a-band (32 GHz) phase measurements were transmitted and received by both satellites. After ground processing the combined measurements provided obtaining the inter-satellite distance free of ionosphere instability [2]. Each of the spacecrafts was equipped with GPS-receivers, altitude sensors, and precision accelerometers.

On 22 May 2018, GRACE project was followed by the launch of two twin-satellites in the framework of the GRACE Follow-On (FO) project [3]. The latter was aimed at providing data flow for monthly global high-resolution models of the Earth's gravity field. It was a continuation of monitoring slow time variations of the Earth's gravity field [4] started in the GRACE project. Two satellites of GRACE FO have the same orbit with an altitude of 500 km (the orbital period is 90 min) at a distance of ∼200 km from each other. The essential difference between GRACE FO and GRACE is that the SCs carry additional tools, namely, a laser interferometric system [5]. Methods of laser interferometry make it possible to measure a distance with very high accuracy and are widely employed in many fields of science and technique from astronomy [6] and gravitational wave detection [7] to surface shape control [8] and medicine [9]. GRACE FO satellites, in addition to microwave devices identical to those in GRACE, are equipped with laser systems based on Nd:YAG lasers emitting at a wavelength of 1064 nm. The error of measuring a distance between satellites in GRACE constellation was ∼1 μm, and in GRACE FO it reached 1 nm [3].

Space laser interferometers utilise transmitter–responder (transponder) technology, which implies that one of the SCs having got a signal from the other SC, does not reflect it backward but sends a signal of another laser, whose phase is locked to the received signal (Fig. 1). Each SC has a similar interferometer with frequency-stabilised laser sources. When the radiation of the master laser on SC1 crosses the inter-satellite distance and reaches SC2, the optoelectronic system of an automatic phase control synchronises the radiation phase of the slave laser SC2 with that of the received weak light signal. Then, the laser radiation of SC2 is directed back to SC1. Information about the length of the light beam double-pass trip is comprised in a phase difference between the SC1 reference beam and received weak light signals. It is the basic operation principle of a transponder-type laser interferometer, which in this case is used as a range finder and measures a distance between two SCs separated from each other by ∼200 km. Such a scheme makes it possible to weaken the requirements to the laser source and increase reliability of system functioning.

Presently, the development and implementation of a native space gravimetry project is actively discussed. Realisation of a laser interferometric system is one of the main directions in this project [10–12]. The present work is a

K.S. Kudeyarov, D.S. Kryuchkov, I.A. Semerikov, K.Yu. Khabarova
P.N. Lebedev Physical Institute, Russian Academy of Sciences, Leninsky prosp. 53, 119991 Moscow, Russia;
e-mail: kost1994@yandex.ru;
V.K. Milyukov Sternberg Astronomical Institute of Lomonosov Moscow State University, Universitetsky prosp. 13, 119234 Moscow, Russia;
O.A. Ivlev Research and Production Corporation 'Precision Systems and Instruments', Aviamotornaya ul. 53, 111024 Moscow, Russia;
N.N. Kolachevsky P.N. Lebedev Physical Institute, Russian Academy of Sciences, Leninsky prosp. 53, 119991 Moscow, Russia; Russian Quantum Center, International Center for Quantum Technologies, Bol'shoi blv. 30/1, Skolkovo Innovation Center Area, 121205 Moscow, Russia

Received 14 March 2022; revision received 24 April 2022
Kvantovaya Elektronika **52** (6) 555–559 (2022)
Translated by by N.A. Raspopov

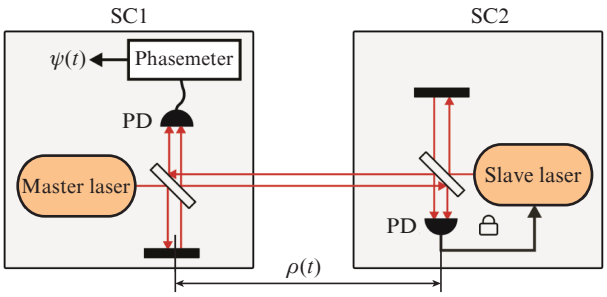

Figure 1. (Colour online) Schematic of measuring displacement with a laser interferometer in a transponder scheme:
(SC1, SC2) spacecrafts; (PD) photodetectors; $\rho(t)$ is the optical path length; $\psi(t)$ is the measured phase signal; 'the lock' denotes phase locking.

step towards this aim. It is intended to demonstrate functionality of principal units of a laboratory interferometer and estimate attainable measurement errors for linear displacements.

2. Heterodyne interferometer

In a laser heterodyne interferometer, the optical beams of reference and signal arms are superposed on a photodetector. A heterodyne signal from the photodetector passes to a phasemeter, which measures a signal phase $\psi(t)$ proportional to a distance from a remote object $\rho(t)$ [5]:

$$\psi(t) \approx -\omega_{\text{offset}}\, t - \frac{4\pi}{\lambda}\rho(t), \tag{1}$$

where λ is the laser source wavelength; and ω_{offset} is the shift of the radiation angular frequency in the interferometer reference arm. This shift may be related to a master laser frequency detuning from that of a slave laser, a Doppler effect due to SC relative motion, etc. In our study, we have elaborated and realised a heterodyne interferometric scheme comprising two enclosed interferometers and two laser beams, each of them passing its own optical path (Fig. 2). This scheme measures linear displacements in the configuration close to the transponder one without creating two full interferometric units with independent laser sources and large-size vacuum chambers. One interferometer measures 'the initial' phase difference of optical beams $\psi_0(t)$, and the other interferometer measures their phase difference $\psi(t)$ after one of the beams reflects from the mirror undergoing a linear displacement. The signal directly related to the linear displacement is obtained by subtracting these two phase signals. The analogy with a transponder scheme is that the phase difference between the beams of two lasers (master and slave) is also detected in two interferometers (see Fig. 1): first, in the SC with the slave laser

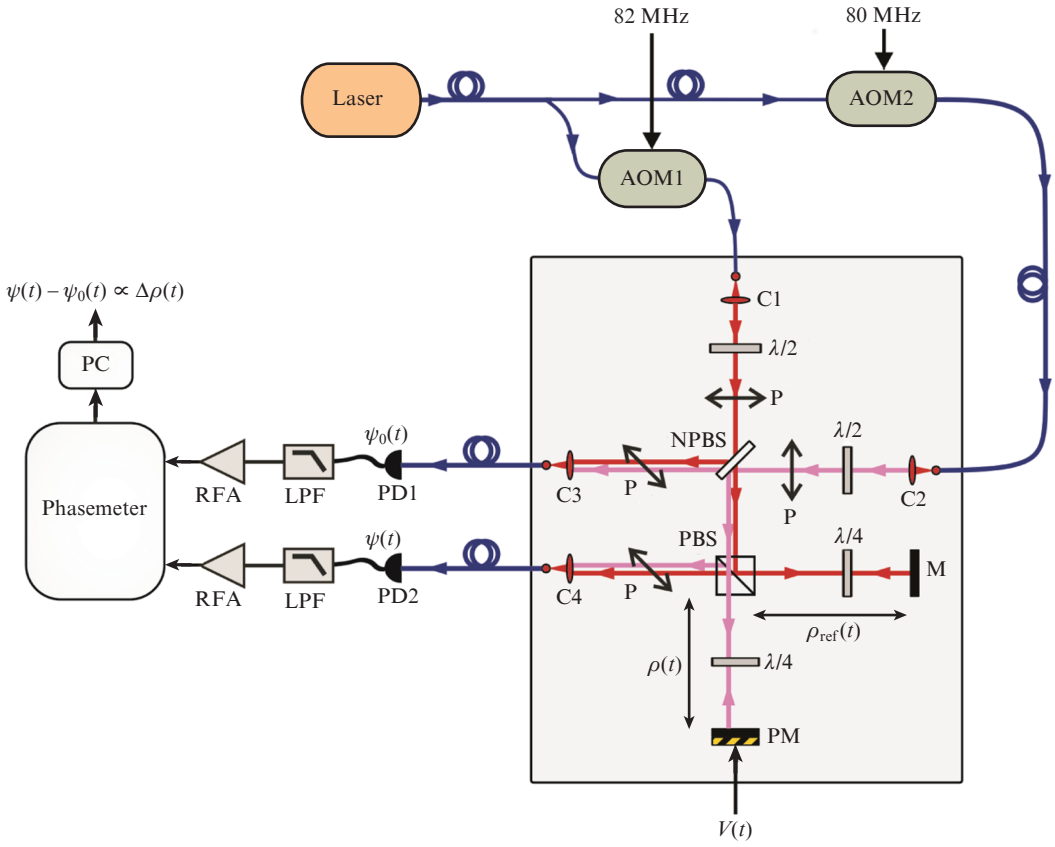

Figure 2. (Colour online) Laboratory model of a heterodyne interferometer:
(AOM1, AOM2) acousto-optic modulators; (C1–C4) collimators; (P) polarisers; (M) mirror; (PM) mirror on a piezoactuator; (NPBS) nonpolarising beam splitter; (PBS) polarising beam splitter; ($\lambda/2$) half-wave phase plates; ($\lambda/4$) quarter-wave plates; (PD1, PD2) photodetectors; (LPF) low-pass filters; (RFA) radio-frequency amplifiers; (PC) personal computer; $V(t)$ is the voltage applied to the piezoactuator; $\rho(t)$ and $\rho_{\text{ref}}(t)$ are the lengths of the signal and reference interferometer arms, respectively; $\psi_0(t)$ and $\psi(t)$ are the measured phase signals; blue colour designates fibre-optic cables, black colour refers to electric signals, red and pink colour marks optical beams.

(for phase locking to the master laser) and, second, in the SC with the master laser (for detecting the linear displacement signal). The scheme used in the present work differs from a transponder one by the absence of phase locking between one laser and the other. However, the scheme can be completed by a phase-locked loop: a signal of the initial phase difference from the first interferometer can be used as a feedback signal applied, for example, to an acousto-optic modulator (AOM).

The source of laser radiation was a cw fibre laser Koheras AdjustIK E15 with a radiation wavelength of 1550 nm, whose frequency was locked to an external silicon resonator [13]. The laser frequency instability may introduce an error $\delta\rho_{\text{las}}$ into displacement measurements, which can be estimated as follows:

$$\delta\rho_{\text{las}} = \frac{\lambda}{4\pi}\delta\psi_{\text{las}} = \frac{\lambda}{4\pi}\frac{\rho - \rho_{\text{ref}}}{L_{\text{coh}}}, \tag{2}$$

where $\delta\psi_{\text{las}}$ is the phase error of laser radiation for the time lapse needed to pass the optical path difference; $\rho - \rho_{\text{ref}}$ is the length difference between interferometer signal and reference arms (that is, the optical path difference); and L_{coh} is the coherence length of the laser radiation source. The laser had a relative frequency instability below 10^{-14} for averaging times of 200 ms–1 s and the coherence length of ~30000 km, which corresponds to a displacement measurement error of 0.1 fm at the path difference in the present work of 2.5 cm (for the orbital path difference of ~200 km, the error would be 0.8 nm).

In the scheme from Fig. 2, a laser radiation with a power of 20 mW was split by a fibre splitter in the ratio 50 : 50 into two beams. Each beam passed through the fibre AOM, which shifted the radiation frequency in one beam by 80 MHz, and in the other beam by 82 MHz. A beat note at the difference frequency ω_{offset} = 2 MHz was observed while detecting the interference of the beams. This was a simulation of the Doppler shift corresponding to a relative velocity of two satellites 1.3 m s^{-1}.

Having passed the AOM, each of the beams passed through a single-mode fibre-optic cable to the interferometer mounted on an optical breadboard and was collimated by an aspheric lens (C1 and C2). Then, for each beam, one of two orthogonal polarisations (horizontal or vertical) was formed by using a half-wave plate $\lambda/2$ and polariser P. Then, the beams from two channels were mixed on a nonpolarising beam splitter 50 : 50 (NPBS). One part of the radiation was directed to a photodetector PD1 recording the heterodyne signal at the frequency ω_{offset} = 2 MHz with the phase

$$\psi_0(t) = -\omega_{\text{offset}}t - \varphi_{\text{in}}(t), \tag{3}$$

where $\varphi_{\text{in}}(t)$ is the phase difference for radiations in two optical beams prior to splitting in the NPBS. In front of the collimator, there was a polariser P transmitting the radiation linearly polarised at an angle of 45° with respect to vertical. In this way, the parts of radiation with similar polarisations were selected from both the beams for observing the interference. The other part of radiation passed to the second interferometer, namely, to a polarisation beam splitter (PBS) with the extinction ratio of greater than 1000 : 1. Since the polarisations in two beams are orthogonal, one of them passes to the reference arm, and the second passes to signal arm. The signal arm length was ~5 cm, and the reference arm length was ~2.5 cm. The mirror was moved by a piezoactuator. Beams in both arms passed through quarter-wave plates $\lambda/4$ and were reflected back. The beams reflected back to the polarisation beam splitter PBS were focused by a collimator C4 onto a photodetector PD2, which detected the heterodyne signal with the phase

$$\psi(t) = -\omega_{\text{offset}}t - \varphi_{in}(t) - \frac{4\pi}{\lambda}[\rho(t) - \rho_{\text{ref}}(t)]. \tag{4}$$

This signal was detected by an InGaAs pin-photodiode with fibre-optic FC/APC connectors. Photodetector signals with a power of approximately –23 dBm at frequencies of about 2 MHz passed a low-pass filter LPF with a cutoff frequency of 2.5 MHz and were amplified in a RF amplifiers RFA by 24 dB. The signal-to-noise ratio in obtained signals was at least 31 dB and was limited by extinction ratio of the employed polarisation optics. Then these signals passed to a digital phasemeter K + K FXE [14] operated in the Λ-regime [15]. This phasemeter has four measuring inputs for signals with frequencies in the range 4 kHz–60 MHz and one reference input for a 10-MHz signal. The reference signal was a signal from a RF oscillator stabilised by a passive hydrogen maser. The phasemeter simultaneously counted the number of cycles in the signal under study for the time corresponding to a definite number of reference signal cycles (similarly to a frequency counter) and measured an analogue phase inside the cycle. This gives a possibility to measure phase shifts in an unlimited range with a high resolution. The intrinsic noise of the phasemeter is studied in Section 3 of the present paper. The phasemeter transmits phase values $\psi_0(t)$ and $\psi(t)$ to a computer (PC), and a displacement of the mirror on a piezoactuator can be calculated by formulae (3) and (4):

$$\Delta\rho(t) = \rho(t) - \rho(0) = \frac{\lambda}{4\pi}[\psi(t) - \psi_0(t)] + \rho_{\text{ref}}(t) - \rho(0). \tag{5}$$

In calculations of displacements from experimental data it was assumed that $\rho_{\text{ref}}(t)$ = const, and not varying terms $\rho_{\text{ref}}(t)$ and $\rho(0)$ were neglected.

For determining the error of measuring linear displacements, it was necessary to minimise the path difference variations in the interferometer not related to piezoactuator motion. One factor affecting the length of interferometer arms was fluctuating laboratory pressure and temperature, which changed the air refractive index. To minimise the influence of this factor, we placed the interferometer into a vacuum chamber with electrical and fibre-optic feedthroughs. In experiments, the vacuum chamber was evacuated by a scroll pump to a pressure of 2×10^{-1} mbar. A higher vacuum in the chamber had no effect on measurement errors. Thermal expansion of the interferometer optical table was minimised by stabilising its temperature with an ohmic heater having the residual oscillations of less than 0.05 K at the averaging time of 5 hours. A general view of the laser interferometer model is shown in Fig. 3.

3. Measurement of linear displacements

At a first stage of the experiment, the maximal possible linear displacement of the mirror was measured. The piezoactuator was driven by a triangular control signal $V(t)$ at a frequency of 0.55 Hz with an amplitude of 75 V. The control signal was recorded simultaneously with data from the digital phaseme-

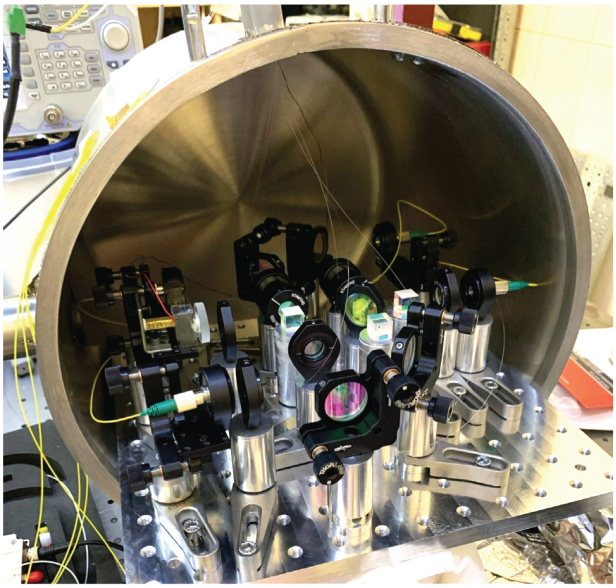

Figure 3. (Colour online) General view of the laser interferometer model (the vacuum chamber is open).

ter. The signal and measurement results are presented in Fig. 4. The maximal displacement was 17.1 μm. The nontriangle shape of the phase signal is explained by a nonlinear hysteresis character of piezoactuator motion [16].

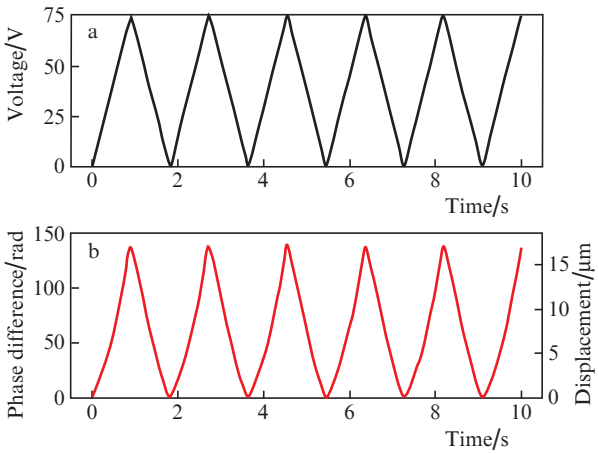

Figure 4. (Colour online) (a) Control signal applied to piezoactuator, and (b) results of phase measurements of mirror shifts [the left scale is the measured phase difference $\psi(t) - \psi_0(t)$, and right scale is the displacement calculated by formula (5)].

The measurement error was estimated by comparing the measured mirror displacement with the nominal shift calculated as a product of the control voltage and average piezoactuator gain k:

$$\Delta\rho_{\text{nom}}(t) = kV(t). \tag{6}$$

The comparison was performed for small displacements of at most 200 nm, because in this range piezoactuator displacements can be considered almost linear. A random control signal was applied to the piezoactuator at an average frequency of 0.1 Hz (Fig. 5). The measurement error was calculated as the difference between the phase measurement result and nominal calculated shift:

$$\delta\rho(t) = \Delta\rho(t) - \Delta\rho_{\text{nom}}(t). \tag{7}$$

In addition, a phasemeter noise was measured by applying a signal from one of the photodetectors to two independent inputs of the phasemeter with following subtraction of phasemeter readings.

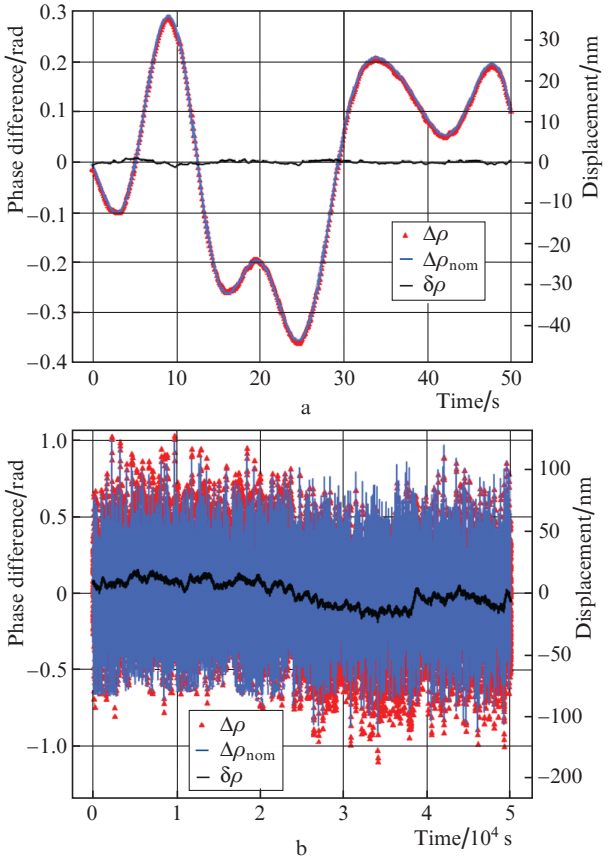

Figure 5. (Colour online) Results of small displacement measurements $\Delta\rho$, nominal values of displacement $\Delta\rho_{\text{nom}}$ calculated by formula (6) and measurement error $\delta\rho$ calculated by formula (7) for the time lapses of (a) 50 and (b) 5×10^4 s.

For the main values characterising errors, we used modified Allan variance [17] and the power spectral density (PSD) of noise calculated by the Welch method [18] (Fig. 6). The error determined by the phasemeter was below 40 pm over the whole range of averaging times, and at the averaging time of $1-4\times10^3$ s it was less than 10 pm. The PSD of the phasemeter noise did not exceed 10^{-5} nm Hz$^{-1/2}$ in the frequency range $10^{-3}-50$ Hz. The total measurement error was 92 pm at the averaging time of 0.1 s, then it increased and reached 8.2 nm at the averaging time of 10^4 s. At the averaging time of 10 s, corresponding to a typical measurement time in an orbit constellation, the error was at most 270 pm. The PSD of noises was $\sim 4 \times 10^{-5}$ nm Hz$^{-1/2}$ in the frequency range 1–50 Hz. In the range 10–50 Hz, the noise spectrum had several narrow peaks caused by the action of vibrations on the interferometer. At frequencies below 1 Hz, the noise PSD increased and reached 2.5 nm Hz$^{-1/2}$ at a frequency of

0.0013 Hz. This measurement error value is most likely related to imperfect calculation of mirror position (at short averaging times) and residual thermal effects, which lead to unaccounted variations of optical trace length (at long times), rather than to fundamental limitations of the measurement system.

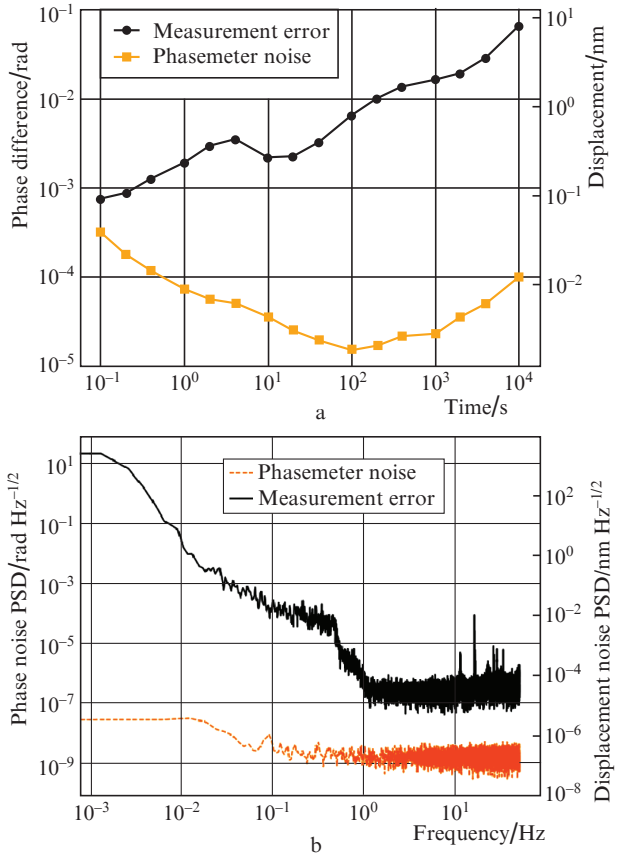

Figure 6. (Colour online) (a) Modified Allan variance, as well as (b) power spectral density of phasemeter noise and displacement measurement error calculated by formula (7). The parameters mentioned were calculated for the measurements from Fig. 5, that is, at small mirror shifts (up to 200 nm).

4. Conclusions

The study shows that the designed laboratory model of the heterodyne interferometer makes it possible to detect linear displacements up to 17.1 μm, which in the order of magnitude corresponds to the measurement range of real displacements in the SC pair of GRACE FO (±25 μm). An estimated error of measuring small linear displacements (up to 200 nm) was ∼270 pm at the averaging time of 10 s and ∼8 nm at averaging time of several hours. In this case, the measured PSD of phase noises of the heterodyne interferometer was at a level corresponding to characteristics of existing orbital laser interferometric systems [3]. The error introduced by a laser frequency instability was negligible. The observed characteristics can be further improved by introducing an additional interferometer to the scheme as an independent sensor of mirror position and by better thermal stabilisation of the vacuum chamber.

The developed model is a simplified variant of a laser interferometric system; however, it comprises the units that correspond to a transponder scheme and allows one to simulate a Doppler frequency shift due to satellite mutual motion. The investigation performed proved the possibility to reach the sensitivity needed for the development of an orbital constellation project. The development of a model closer to real conditions requires the addition of such units as a system for stabilising an optical beam direction and system for locking the phase of one laser to the radiation of the other laser; also, the optical path length should be enlarged.

Acknowledgements. The work was supported by the Russian Foundation for Basic Research (Grant Nos 20-32-90044 and 19-29-11008).

The authors are grateful to M.M. Khudyakov for the help in designing a fibre-optic vacuum feedthrough.

References

1. Tapley B.D., Bettadpur S., Watkins M.M., Reigber Ch. *Geophys. Res. Lett.*, **31** (9), L09607 (2004).
2. Dunn C., Bertiger W., Bar-Sever Y., et al. *GPS World*, **14**, 16 (2003).
3. Abich K., Abramovici A., et al. *Phys. Rev. Lett.*, **123** (3), 031101 (2019).
4. Flechtner F., Neumayer K.-H., et al. *Surv. Geophys.*, **37** (2), 453 (2016).
5. Sheard B.S., Heinzel G., et al. *J. Geodesy*, **86** (12), 1083 (2012).
6. Monnier J.D. *Rep. Prog. Phys.*, **66** (5), 789 (2003).
7. Abbott B.P., Abbott R., et al. *Rep. Prog. Phys.*, **72**, 113 (2009).
8. De Groot P. *Adv. Opt. Photonics*, **7** (1), 1 (2015).
9. Nolte D.D. *Optical Interferometry for Biology and Medicine* (New York: Springer, 2012).
10. Shchipunov A.N., Tatarenkov V.M., Denisenko O.V., et al. *Meas. Tech.*, **57**, 1228 (2015).
11. Prilepin M.T., Andreev V.Yu., Grigor'evskii V.B., et al. *J. Commun. Technol. Electron.*, **54**, 73 (2009) [*Radiotekh. Elektron.*, **54**, 78 (2009)].
12. Minin I.B., Shevchenko V.M., Dubrov M.N. *Proc. 2019 IEEE 8th Int. Conf. on Advanced Optoelectronics and Lasers (CAOL)* (Sozopol, Bulgaria, 2019) pp 220–224.
13. Vishnyakova G.A., Kryuchkov D.S., Zhadnov N.O., et al. *AIP Conf. Proc.*, **2241**, 5 (2020).
14. Kramer G., Klische W. *Proc. 2001 IEEE Int. Frequncy Control Symp. and PDA Exhibition* (Seattle, USA, 2001) pp 144–151.
15. Benkler E., Lisdat C., Sterr U. *Metrologia*, **52** (4), 565 (2015).
16. www.thorlabs.com/drawings/a9a1a8b333b2ec5b-60E8763A-AC90-F1C6-D49F1B34A9979B85/PK2FQP2-SpecSheet.pdf.
17. Allan D.W., Barnes J.A. *Proc. Thirty Fifth Annual Frequency Control Symp.* (Philadelphia, USA, 1981) pp 470–475.
18. Welch P. *IEEE Trans. Audio Electroacoust.*, **15**, 70 (1967).